Electron Bernstein wave heating via the slow X-B mode conversion process with direct launching from the high field side in LHD

H. Igami 1), Y. Yoshimura 1), S. Kubo 1), T. Shimozuma 1), H. Takahashi 1), T. Akiyama 1), C. Takahashi 1), K. Nagaoka 1), T. Minami 1), K. Matsuoka 1), S. Okamura 1), H. Tanaka 2), K. Nagasaki 3), S. Inagaki 4), T. Mutoh 1), A. Komori 1), the LHD experimental group 1) and the CHS experimental group 1)

1) National Institute for Fusion Science, Japan
2) Graduate School of Energy Science, Kyoto Univ., Japan
3) Institute of Advanced Energy, Kyoto Univ., Japan
4) Research Institute for Applied Mechanics, Kyusyu Univ., Japan
e-mail contact of main author: igami@LHD.nifs.ac.jp

Abstract. In the large helical device (LHD), direct oblique launching of the extraordinary (X-) mode from the high magnetic field side is available without installation of any additional mirror or installation of a launcher in the inner side of the torus. The launched X-mode first encounters the electron cyclotron resonance (ECR) layer from the high magnetic field side and then approaches the upper hybrid resonance (UHR) layer where mode conversion from the X-mode to electron Bernstein wave (EBW) occurs. Complete power absorption with a finite parallel component of the refractive index is promising whether the launched wave power is absorbed as the electromagnetic X-mode or is absorbed as electrostatic EBW even in the peripheral region. In the experiment, strong power absorption has been observed by direct oblique launching of the X-mode. Observation of the parametric decay wave suggests a fraction of the launched power reached the UHR layer that is located near the plasma boundary. The result of numerical analysis with three dimensional ray-tracing calculation using the dispersion equation in hot plasmas suggests that the launched X-mode is refracted toward the magnetic axis and strongly absorbed very close to the ECR layer that is located around $\rho \sim 0.5$. The main part of the launched power is absorbed as the X-mode in the ECR layer where the electron temperature is sufficient high, while a fraction of the power reaches the UHR that is located in almost the plasma boundary.

1. Introduction

Since Electron Bernstein wave (EBW) is an electrostatic mode, it is required to be excited in the upper hybrid resonance (UHR) layer via the mode conversion process from the slow extraordinary (SX-) mode that propagates in the higher field side of the UHR layer. Once the EBW is excited, it can propagate toward the ECR layer without the density limit and strongly absorbed by the cyclotron damping even in the low density/temperature region. Therefore electron cyclotron heating (ECH) and current drive (ECCD) by EBW is expected as a promising substitute for conventional ways of ECH/ECCD using electromagnetic (EM) modes, in the inner region of over-dense plasmas where EM mode cannot propagate, and/or in the low density/temperature region where the absorption of EM mode is weak. Since the UHR layer is shielded by the evanescent region lying between the right handed cyclotron cutoff (RC) and the UHR layer, the X-mode cannot access the UHR layer directly with launching from the low magnetic field side. Therefore getting accessibility of the X-mode to the UHR layer is an important and complex issue for ECH/ECCD using EBW. One straightforward way is launching the X-mode toward the UHR layer from the high magnetic field side. However, if one expects the single path absorption of the launched wave without suffering multiple reflections, this way usually requires an installation of the final mirror antenna in the inner side of the torus for toroidal plasmas [1][2][3].
In the magnetic configuration of the large helical device (LHD), direct launching of the SX-mode from the high field side is available. Two existing antennas installed in a bottom port of the vacuum vessel can be used for this purpose without any installation of additional final mirror [4]. This method has flexibility of wave propagation angle therefore it may be

beneficial for local heating and current drive in over-dense core regions and/or low temperature peripheral regions. The launched wave propagates obliquely to the external magnetic filed and accesses the ECR and the UHR layers in the peripheral region ($\rho > 0.7$, where ρ is the normalized minor radius.) if the trajectory of the launched wave is almost straight. Generally it is said that for wide range of the electron density, the absorption of the fundamental X-mode is weak in the case of perpendicular propagation whereas it becomes very strong in the case of oblique propagation [5][6]. If the electron temperature is sufficient low where the X-mode encounters the ECR layer, the oblique X-mode has an opportunity to reach the UHR layer without being damped out and to excite EBW. Even if the X-mode wave is completely damped out in the ECR layer, this launching method remains to be beneficial for off-axis ECH/ECCD in the low density/temperature peripheral region and can be expected as a control knob of various phenomena which occur in the peripheral region. We have carried out the direct launching experiments in hope of EBW excitation. The lower hybrid (LH) wave is excited via the nonlinear three wave coupling process in the UHR layer by the pumping X-mode wave. In the experiment, significant power absorption has been observed. In the experiment, frequency spectrums of the parametric decay wave were observed in the frequency range of the LH wave.

In this paper, the experimental configuration and the results are reported in section 2. The numerical analyses of the experimental data using the ray-tracing calculation are presented in section 3. Discussion about the regime of the heating and summary will be presented in section 4.

2. Experimental configuration and results

2.1. Absorption profile obtained with direct launching from the high magnetic field side

FIG.1 shows an oblique cross section of LHD along the incident wave vector in a magnetic configuration (R_{ax}, B_{ax}) = (3.6m, 2.75T), where R_{ax} is the position of the magnetic axis from the center of the torus and B_{ax} is magnetic field strength at the magnetic axis. The 84GHz electron cyclotron (EC) wave was launched from one of the existing antennas installed in a bottom port of the vacuum vessel. The launched EC wave first encounters the ECR layer in

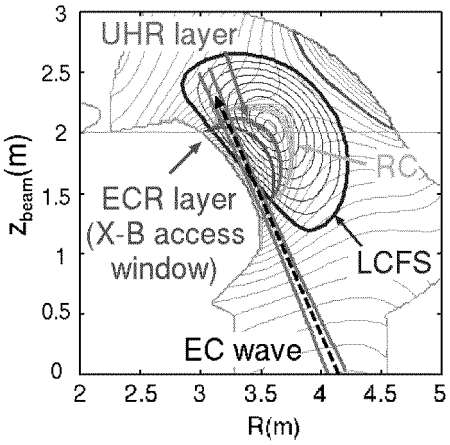

FIG.1 : An oblique cross section of LHD along the incident EC-wave vector. The wave can access the UHR layer through the ECR layer, that is X-B access window.

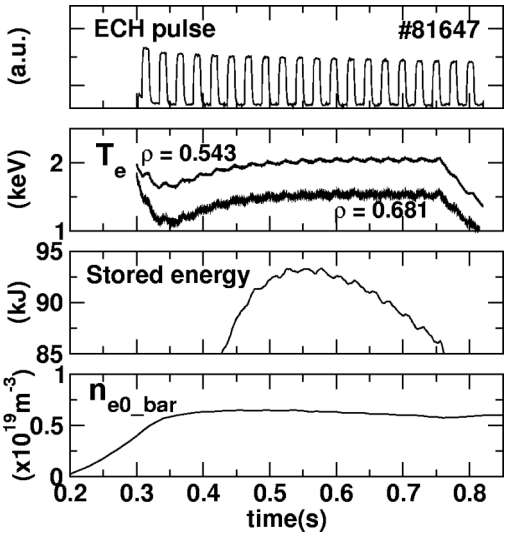

FIG.2: Typical set of discharge waveforms when the X-mode was launched as shown in FIG 1. The temperature and the stored energy increase with the modulated ECH pulse.

the outer side of the last closed flux surface (LCFS), thus the wave can pass though this outer ECR layer without absorption and can break into the plasma from the high field side without being shielded by the right handed cyclotron cut-off (RC). The wave can approaches the ECR layer again from the high field side. If the cyclotron damping as an EM mode is weak, the wave can pass though this inner ECR layer, that is X-B access window, then reaches the UHR layer. *FIG.2* shows a typical set of the discharge waveforms when the X-mode was launched with 39Hz, 100% power modulation. The central electron density was $0.6\text{x}10^{19}\text{m}^{-3}$, that is less than the cutoff density and the central electron temperature was more than 2keV. The stored energy and the electron temperature around $\rho\sim0.5$ significantly increased with the modulated ECH pulse. The fast Fourier transform (FFT) analysis of the electron temperature signals is a powerful tool for finding the power absorption region when the EC wave is launched with power modulation.

FIG.3 shows the profiles of 39Hz perturbation amplitude and the profiles of the phase delay from the modulated ECH pulse obtained by FFT analysis of the electron cyclotron emission (ECE) signals. Since the toroidal aiming point "T_f" is the same but the radial aiming point "Rf" is different in each case of (a)-(c), the launched wave vectors lie on the same oblique cross section presented in *FIG.1*, but aiming different radial directions. As "R_f" becomes large, the aiming point moves from the region that is very close to the inner vacuum vessel toward the magnetic axis. Note that in every case of (a)-(c), the launched wave approach the ECR layer, i.e. the X-B access window from the high field. In the cases of (a) and (b), three

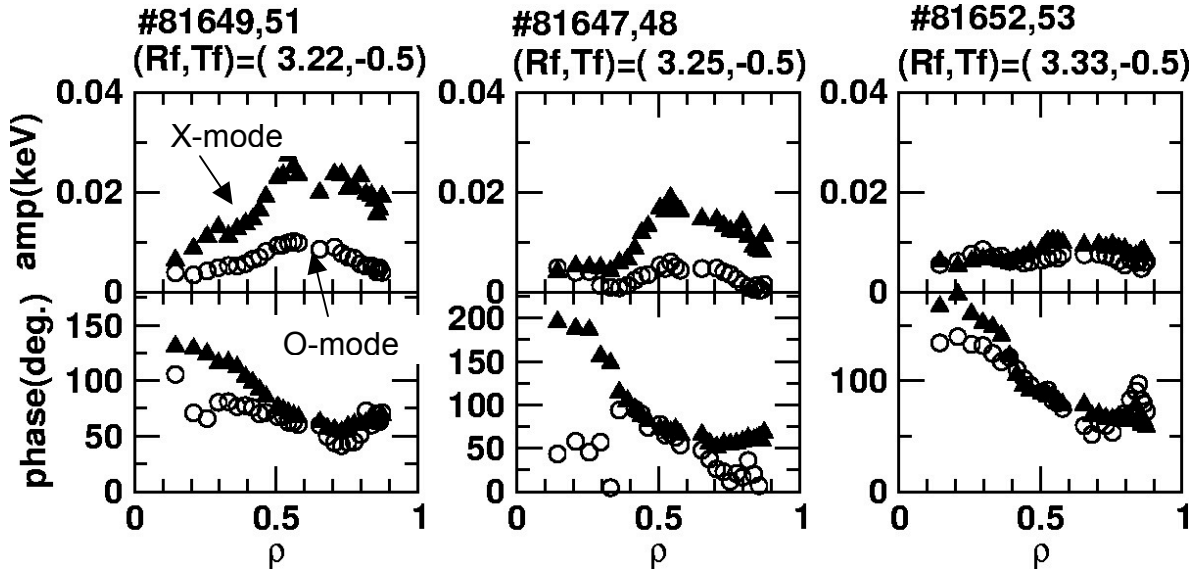

FIG.3: Profiles of 39Hz perturbation amplitude and phase delay from the modulated ECH pulse for different cases of launching direction. They are obtained by FFT analysis of ECE signals. The launched wave vectors lie on the same oblique cross section presented in FIG. 1 since the toroidal aiming point "Tf" is the same. As the radial aiming point "Rf" becomes large, the straight outgoing line of the incident vector moves to the magnetic axis from the inner wall of the vacuum vessel. The Black triangles show the cases of the X-mode injection and the white circles shows the cases of the O-mode injection. The dashed lines indicate the cross points of the straight outgoing line and the ECR layer.

sets of the peak of amplitude and the bottom of the phase delay can be seen where $\rho\sim0.2$, 0.5 and 0.7 with the X-mode launching, that is to say, power absorption occurs in these three regions. Since the electron density was less than the cutoff density, there are two possible heating regimes, those are, the power absorption as the X-mode and the power absorption as the mode converted EBW. Discrimination between these regimes will be presented by the

numerical analysis of the wave trajectory and the absorption. While, there are no clear sets of the peak and the bottom in any cases of (a)-(c) with the O-mode launching. The profiles of perturbation amplitude are similar with each other. There profiles for O-mode launching may be explained as follows. The power absorption as the fundamental O-mode that propagates obliquely to the external magnetic filed is weak in the peripheral region, thus the launched O-mode passed through the ECR layer and reached the wall of the vacuum vessel, then was reflected. Some part of the wave power might be absorbed after multiple reflections.

2.2. Observation of the parametric decay instability

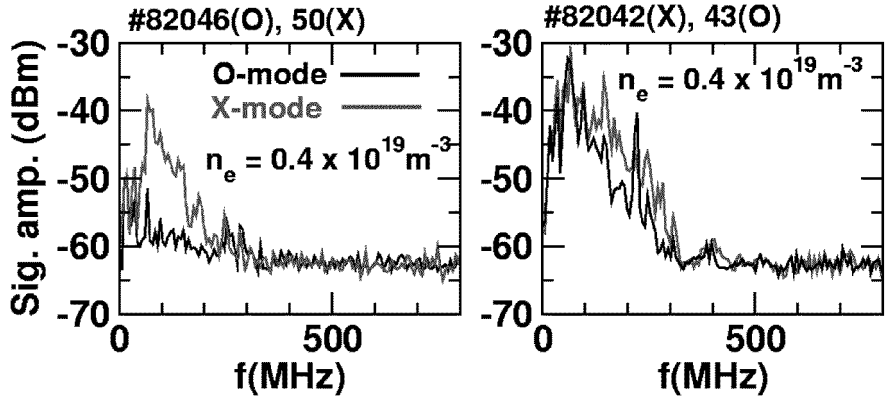

FIG.4: *Spectrums in lower hybrid wave frequency range. (a): Perpendicular launching, for usual ECH. (b) : Oblique launching in the same setting as the case of FIG.3-(b). Sensitivity calibration for each frequency is not done.*

The nonlinear three wave coupling process occurs in the UHR layer if the amplitude of driving X-mode wave is large [6][7][8]. Measurement of the parametric decay wave that is excited in this three wave coupling process was carried out in the lower hybrid frequency range with use of an antenna originally installed for ion cyclotron resonance frequency (ICRF) heating. For comparison, frequency spectrums shown in *FIG. 4-(a)* were obtained when X, and O-mode were launched almost perpendicularly toward the fundamental ECR layer near the magnetic axis. Since the O-mode is well absorbed in this launching condition, only very weak spectrum was obtained. The X-mode is reflected at the RC in this launching condition, it may suffer multiple reflections. Some part of the waves might approach the UHR layer from the high field side as the X-mode and may induce the parametric instability. *FIG.4*-(b) shows the spectrums when the X and O-mode were launched toward the same direction as the case of *FIG.3*-(b). A stronger spectrum was obtained with the X-mode launching than the O-mode launching. It suggests at least a part of the launched X-mode reaches the UHR layer without being completely damped out at the ECR layer. *FIG.5* shows the frequency of the lower hybrid wave excited in by the pump wave of 84GHz in the UHR layer. Significant spectrums were observed in the frequency range less than 400MHz. Note that in the frequency range more than 500MHz, the sensitivity of the ICRF antenna becomes worse, therefore significant spectrum could not be obtained even if waves of the range were excited. At least, it can be said that the interactions occur in very low density region where $(\omega_{pe}/\omega)^2<0.045$, where ω_{pe} is the plasma frequency. *FIG.6* presents the model profiles of the normalized density and the electron temperature that agree well with the profiles obtained in the experiment by Thomson scattering measurement. The region where $(\omega_{pe}/\omega)^2<0.045$

coincide with the region where ρ > 0.9. The electron temperature is less than 650eV in the region.

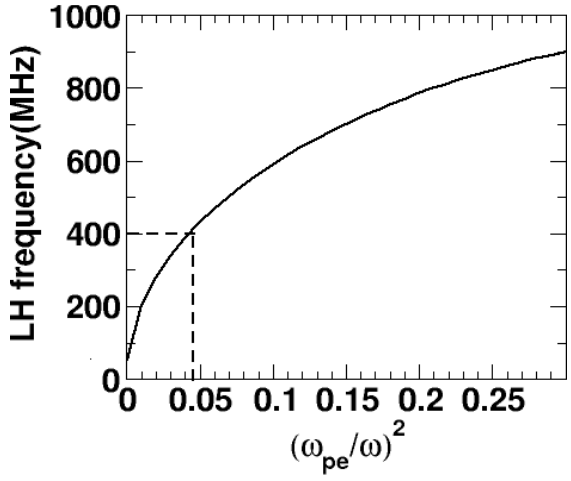

FIG.5 : Frequency of the lower hybrid (LH)wave excited in the UHR layer by the 84GHz pump wave. Pure hydrogen plasma is considered. The LH frequency is plotted as a function of $(\omega_{pe}/\omega)^2$ that is proportional to the electron density. The range where the LH frequency is less than 400MHz corresponds to the range where $(\omega_{pe}/\omega)^2 < 0.045$

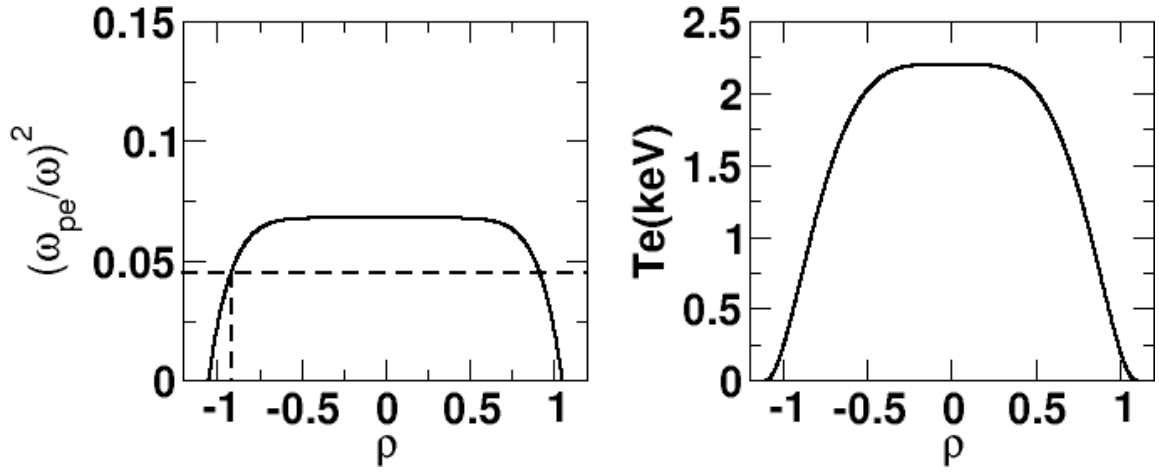

FIG.6 : Profiles of the normalized density (left) and the electron temperature(right), which agree well with the profiles obtained by Thomson scattering measurement. The region where $(\omega_{pe}/\omega)^2 < 0.045$ corresponds to the region where ρ >0.98

3. Numerical analysis on the experimental data

3.1 Ray tracing using the dispersion equations in hot plasmas for EM mode and EBW

The ECR layer and the UHR layer are located very close to each other in our experimental configuration. The finite temperature effect is not negligible between these resonance layers. Therefore it is appropriate to use the dispersion equation of the electromagnetic waves in hot plasmas [9] in the ray-tracing calculation to obtain the orbit correctly [10][11][12]. In the 3-D ray tracing code for LHD configuration [13], we solve the dispersion equation presented in Ref. [9] in the region where $(\omega_{pe}/\omega)^2>0.02$. At the boundary of the plasma, initial solution of the dispersion equation is given by the cold plasma approximation, then the equation to be solved is switched to the dispersion equation in hot plasmas at the point where $(\omega_{pe}/\omega)^2 =$

0.02. The absorption coefficient and the normalized absorbed power are obtained as following equations.

Absorption coefficient : $\alpha = 2\, G_I(k,\omega)]/(dG_R/d\mathbf{k_R})^{1/2}$ (1)
Optical depth : $\tau = \Sigma\, \alpha ds$ (ds is the step length.) (2)
Normalized absorbed power : $P_{abs}/P_{inj} = 1 - \exp(-\tau)$ (3)

Where, G_R is the real part and G_I is the imaginary part of the complex dispersion equation G. and $\mathbf{k_R}$ is the real part of the wave vector. P_{abs}/P_{inj} is the absorbed power normalized by the launched power. The dispersion equation in hot plasmas is switched to that of EBW [14] after the ray passes through the ECR layer and the perpendicular component of the refractive index becomes large near the UHR layer.

3.2 Result of the calculation

For the numerical analysis, we used the model profiles presented in *FIG. 6*. The launching condition is the same as the case of *FIG.*3-(b). In *FIG.*7, the result of the calculation for the central code of the incident Gaussian beam of the X-mode is presented. The orbit is refracted toward the magnetic axis. The incident X-mode encounters the ECR layer around ρ~0.55 and is strongly absorbed there. The region where the absorption occurs corresponds to the highest peak point of the amplitude profile shown in *FIG.*3-(b).

4. Discussion and summary

With the direct oblique launching of the X-mode from a bottom port in hope of EBW excitation, significant power absorption was observed mainly around ρ~0.5. The parametric wave was observed in the similar experimental configuration. However, the observed frequency spectrum suggests that the nonlinear three wave coupling process occurred in the region where ρ >0.9. In the ray tracing calculation using the hot plasma dispersion equation, the launched X-mode along the central code of the Gaussian beam is refracted toward the magnetic axis and is strongly absorbed and damped out in the ECR layer around ρ~0.55 as the electromagnetic X-mode before it reaches the UHR layer. One possible way that the launched X-mode can reach the UHR layer near the plasma boundary is to suffer multiple reflections. Possibility that a part of the launched power of the X-mode reaches the region directly, then the excited EBW is absorbed, is still remained since the incident Gaussian beam has width to some extent. Anyhow, with direct oblique launching from the high field side with the existing bottom antenna, efficient off-axis heating at large parallel component of the refractive index ($N_{//} \sim 0.5$) is possible in the LHD configuration. Application of this injection method can be expected as an efficient way of off-axis heating and current drive.

Acknowledgment

The authors appreciate the technical staff of ECH and LHD for their great efforts to perform the experiment. These works were mainly performed under the budget codes NIFS07ULRR501-3,518, NIFS07KLRR303 and partially supported by a grant-in-aid for scientific research of MEXT JAPAN, 2008 19740347.

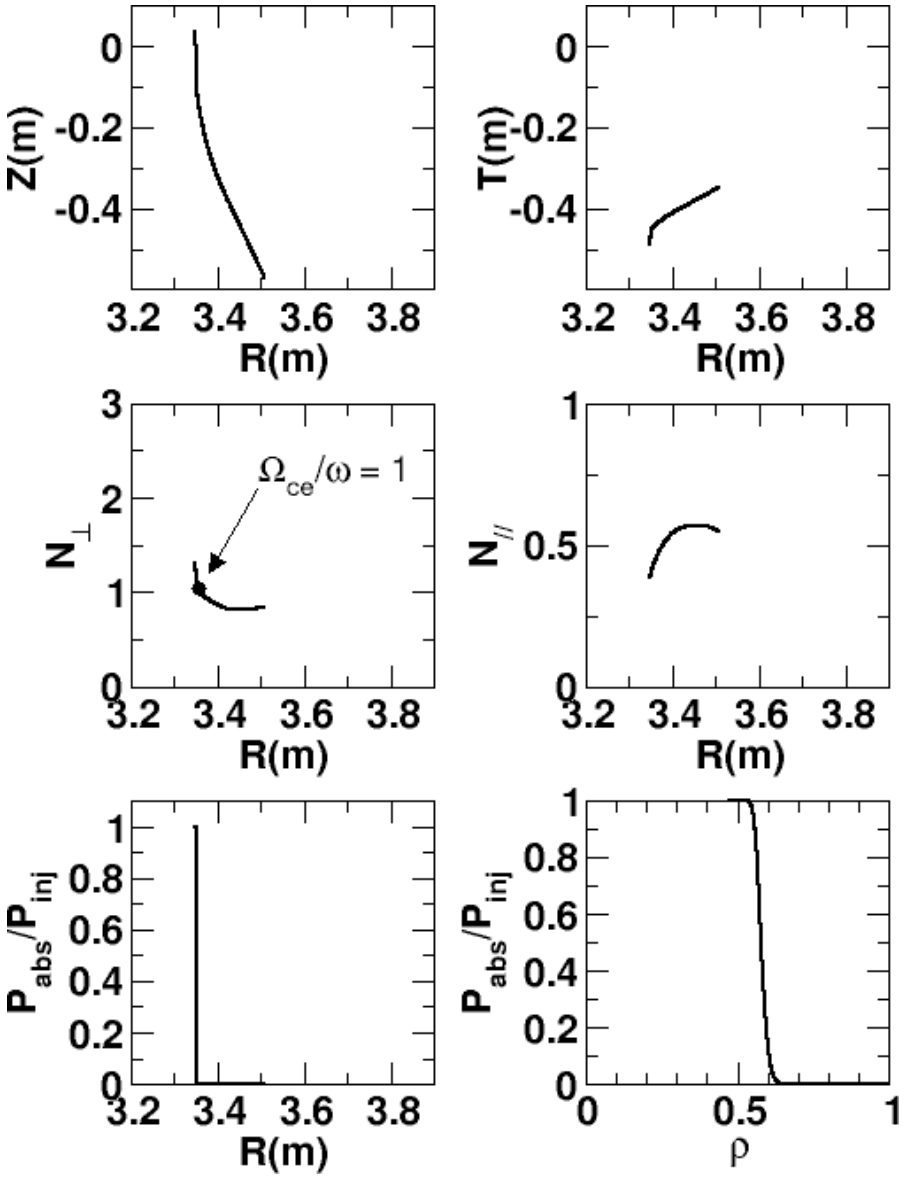

FIG.7: Ray trajectory of the central code of the incident Gaussian beam of the X-mode is plotted. Where "R" is the major radius, "Z" is the vertical direction and "T" is the toroidal direction. The perpendicular and the parallel components of the refractive index are plotted versus the major radius, R(m). The absorbed power normalized by the launched power is plotted as a function of the major radius, R(m) and the normalized minor radius ρ.

References

[1] T. Maekawa, T. Kobayashi, S. Yamaguchi et al., Phys. Rev. Lett. **86**, 3783 (2001)
[2] V. Shevchenko, Y. Baranov, M. O'Brien, and A. Saveliev Rev. Lett. **89**, 265005 (2002)
[3] Y. Yoshimura, K. Nagasaki, T. Akiyama et al., Plasma and Fusion Res **1** (2006) 053
[4] H. Igami, T. Shimozuma, S, Kubo, K. Nagasaki et. al., Plasma and Fusion Res. **1** (2006) 052
[5] M. Bornatici, R. Cano, O. De Barbieri, and F. Engelmann Nucl. Fusion . **23**, 1153 (1983)
[6] V. Erckmann and U. Gasparino Plasma Phys. Control Fusion **36** 1869 (1994)
[7] P.K. Shukla, R. Fedele and U. de Angelis Phy. Rev. A **31** 517 (1985)
[8] F. S. Mc Dermott, K. E. Bekefi, J. S. Levine and M. Porkolab Phys. Fluids **25** 1488 (1983)
[9] A.I. Akhiezer, I. A. Akhiezer, R. V. Polovin, A. G. Sintenko and K. N. Stephanov : *Plasma Electrodynamics* (Pergamon Press) (1975) Chap.5
[10] M. Tanaka, M. Fujiwara and H. Ikegami J. Phys. Soc. Jpn. **50** 1358
[11] E. Westerhof, Plasma Phys. Control. Fusion **39**, 1015 (1997)
[12] M. D. Tokman, E. Westerhof and M.A. Gavrilova, Plasma Phys. Control. Fusion **42**, 191 (2000)
[13] S. Kubo et. al., Journal of Plasma Fusion Research SERIES **5**, 584 (2002)
[14] T. Maekawa, S. Tanaka, Y. Terumichi and Y. Hamada J. Phys. Soc. Jpn. **48** 247 (1980)